**Patterns of river influence and connectivity among subbasins of Puget Sound, with application to bacterial and nutrient loading**

N.S. Banas[1], L. Conway-Cranos[2], D.A. Sutherland[3], P. MacCready[4], P. Kiffney[5], M. Plummer[5]

1. Joint Institute for the Study of the Atmosphere and Ocean, University of Washington, Seattle, WA 98195
2. NOAA contractor, Northwest Fisheries Science Center, National Oceanographic and Atmospheric Administration, 19 2725 Montlake Blvd E. Seattle, WA 98122
3. Department of Geological Sciences, University of Oregon, Eugene, OR 97403
4. School of Oceanography, University of Washington, Seattle, WA 98195
5. Northwest Fisheries Science Center, National Oceanographic and Atmospheric Administration, 19 2725 Montlake Blvd E. Seattle, WA 98122

**Abstract:**

Puget Sound is an estuarine, fjordal inland sea fed by 14 major rivers and also strongly influenced by the Fraser River, which lies outside Puget Sound in the greater Salish Sea. A comprehensive, particle-based reanalysis of existing numerical simulations of 2005–2006 Puget Sound circulation was used to map the area of influence of each of these rivers over a typical seasonal cycle. In the new analysis, 189,000 particles were released in 15 rivers and tracked in three dimensions, including vertical diffusion. Each particle was associated with a freshwater volume, a nutrient load, and a fecal coliform load based on the statistics of ten years of Washington Department of Ecology monitoring data. Simple assumptions regarding mortality and nutrient utilization/export rates were used to estimate the decrease in bacterial and nutrient load as individual parcels of river water age. Reconstructions of basin-scale volume fluxes and salinities from the particle inventory were used to provide consistency checks on the particle calculation. Results suggest that river contributions to total freshwater content in Puget Sound are highly nonlocal in spring and summer, with distant, large rivers (the Fraser and Skagit) accounting for a large fraction of total freshwater. However, bacterial mortality and nutrient export rates are relatively fast compared with transport timescales, and so significant loadings associated with major rivers are in most cases only seen close to the river mouths. One notable exception is fecal coliform concentration in Bellingham Bay and Samish Bay, which lie north of

Puget Sound proper; there, it appears that the Fraser River may rival the local rivers (the Samish and Nooksack) as a pathogen source, with the much higher flow volume of the Fraser compensating for its remoteness.

## Introduction

Puget Sound, Washington, USA is a large, estuarine inland sea composed of a number of fjordal subbasins (Fig. 1). Compared with most large, temperate estuaries its biogeochemistry is highly marine dominated: 70% of dissolved nutrients come from the Pacific via the Strait of Juan de Fuca (Mackas and Harrison 1997, Mohamedali et al. 2011). Nevertheless, there is significant policy and management interest in understanding watershed contributions of environmental stressors, among them nutrient loading in relation to recurrent hypoxia in some subbasins (Newton et al. 2011), and pathogen and pollutant impacts on commercial, recreational, and tribal shellfish harvesting. Overall seasonal and spatial patterns of total river water distribution—i.e., salinity—are well mapped, through a combination of monitoring and modeling (references below). What remains unclear—not just in Puget Sound, but in complex estuarine systems in general—is whether the influence of many rivers of varying magnitude on many basins of varying morphology and connectivity should be thought of as local or nonlocal. Does the Samish River, to pick one example, control water quality in Samish Bay (Fig. 1), or are more distant rivers also important? Conversely, is the nutrient and pathogen load of the Samish River (Swanson et al. 2008) of concern only in Samish Bay, or over a wider area? Questions like this arise throughout Puget Sound, and are crucial to linking marine impacts to land-use management and policy. This paper uses a comprehensive, particle-based reanalysis of an existing hydrodynamic model (Sutherland et al. 2011) to systematically address the question: *which watershed is responsible for freshwater, nutrients, and pathogens found in a given area of Puget Sound at a given time?* In other words, what is the nature of the connectivity between watersheds and subbasins?

This is a thornier question in Puget Sound than in many estuaries because the largest sources of freshwater lie seaward of most of the Sound, whereas almost all the classic theories of estuarine circulation start from the premise of a linear system with a river at one end and saltwater at the other. The largest source of freshwater in the region, the Fraser (mean flow 2200 $m^3\ s^{-1}$), lies ~100 km outside Puget Sound to the north (Figs. 1, 2). Accordingly, Puget Sound is

in many ways a tributary to the Fraser–Strait of Georgia–Strait of Juan de Fuca system,[1] similar to the subestuaries of Chesapeake Bay (Pritchard and Bunce 1959, Pritchard and Carpenter 1960), or the small Gulf Coast estuaries adjacent to the Mississippi River (e.g., Schroeder et al. 1992). Furthermore, within Puget Sound proper, two thirds of total gauged river input (Table 1) enters via Whidbey Basin, close to the Sound's primary and secondary outlets (Admiralty Inlet and Deception Pass), whereas very little freshwater enters via the landward reaches of southern Hood Canal and South Sound (Fig. 1). Past modeling and observations have left open the question of the extent to which the Fraser and Skagit influence the landward reaches of Puget Sound, a question we address below.

Sutherland et al. (2011) documented a high-resolution numerical model of Salish Sea circulation and a skill assessment of this model using an extensive database of temperature, salinity, and current observations. This paper describes a follow-on analysis this model, in effect a post-hoc conversion of a full, three-dimensional representation of an annual cycle in Puget Sound from an Eulerian to a Lagrangian frame. This conversion provides a wealth of additional information at the cost of introducing new numerical biases. Our purpose is to address the central question raised above (which watershed is responsible for river-borne stressors found at a given place and time?) at the system-wide scale. Details of nearshore and intertidal processes are elided. Inputs from the largest 14 Puget Sound/central Salish Sea rivers and the Fraser River are considered, and wastewater treatment plants, non-point sources discharging directly into the Sound, and contributions from more distant rivers like the Columbia (Hickey et al. 2010) are not included. Thus this analysis can provide an attribution of only a portion of the total nutrient and pathogen load to Puget Sound. Our focus is the major rivers, and nutrients and pathogens are discussed here primarily to illustrate that connectivity patterns for river-borne stressors with short decay or utilization times may be very different than the pattern for river water itself. Our central result is that river contributions to total freshwater content in Puget Sound are highly nonlocal, but that the influence of bacterial and nutrient loading by the same rivers is much more local.

---

[1]. Puget Sound, the Strait of Georgia, and the Strait of Juan de Fuca together constitute the Salish Sea. We have included Bellingham, Samish, and Padilla Bays in our analysis (Fig. 1), although these bays, along with the San Juan Islands and Semiyahoo and Birch Bays to the north, are not part of Puget Sound proper, which ends at Admiralty Inlet and Deception Pass (Fig. 1). Where necessary, we distinguish these in the text as the "central Salish Sea."

## Methods

*The circulation model*

The circulation model used here, described in detail by Sutherland et al. (2011), is implemented using ROMS (Regional Ocean Modeling System) in a domain covering the entire Salish Sea and the adjacent coastal ocean from central Oregon to central Vancouver Island (45–50°N, 122–127°W: Fig. 1a). There are 20 terrain-following layers in the vertical, and horizontal resolution ranges from 280 m in southern Puget Sound to 3.1 km far offshore. Bathymetry for Puget Sound is from Finlayson 2005, at 183 m resolution. Wetting and drying of intertidal areas is not included.

The model was run with a baroclinic timestep of 30 s for two yearlong hindcasts, 2005 and 2006, with output saved hourly. These hindcasts were forced by realistic tides, wind and heat fluxes from the MM5 regional forecast model (Mass et al. 2003), open-ocean boundary conditions from the Navy Coastal Ocean Model (Barron et al. 2006, 2007), and streamflow from 16 rivers, the 15 considered in this study (Table 1) and the Columbia. Streamflow was taken from USGS and Environment Canada gauges on all rivers except the Dosewallips and Duckabush, which are ungauged. Flow time series for these small Hood Canal rivers were set equal to that for the nearby Hamma Hamma (Fig. 1) based on their watershed similarities (Table 1).

Sutherland et al. (2011) presents an extensive statistical assessment of model skill, based on comparisons with tide gauges, repeat salinity and temperature profiles, and velocity time series in Puget Sound, the greater Salish Sea, and the continental shelf. The model captures the seasonal cycle of stratification in Puget Sound (an indirect indicator of the accuracy of the tidally averaged estuarine circulation) with no measurable bias, although the model is slightly overstratified in the Strait of Juan de Fuca. It reproduces the seasonal cycle of Puget Sound surface temperature with $r^2 = 0.79–0.95$ at seven of eight repeat hydrographic stations sampled monthly by the Washington Department of Ecology (DOE). For surface salinity at the same stations, $r^2 = 0.51–0.89$. Overall, model skill is best in the eastern Strait of Juan de Fuca and worst in Hood Canal and South Sound, most likely because of the difficulty of balancing model accuracy and model stability in steep topography in narrow channels that are only

marginally resolved (< 10 grid cells across).

*Particle tracking*

Virtual particles were released once per hour at the mouths of 15 rivers (Fig. 1) throughout the two yearlong model hindcasts, 2005 (used here mainly as a spinup period) and 2006 (the analysis period), 131,000 per model year. The 2005 particles were tracked to the end of the year and the 58,000 that remained in the Salish Sea at the end of the run were restarted at the beginning of the 2006 run. Thus the results below are based on 58,000 particle trajectories at the beginning of Jan 2006, increasing to 58,000 + 131,000 = 189,000 at the end of 2006 (see Fig. 5a below). Particle trajectories were sampled at 3 h intervals to produce timeseries of instantaneous inventories, which then were aggregated and averaged in a number of different ways (see Results).

Particles were released at the surface but tracked in three dimensions. Advection was calculated using velocities interpolated from hourly saved ROMS fields, using the midpoint method for timestepping and a timestep of 400 s. Spatial interpolation of velocities was done using one-dimensional linear interpolation within grid cells (Wolk 2003): since this method matches how ROMS discretizes the continuity equation, it preserves mass conservation better than a higher-order interpolation scheme. Vertical diffusion was calculated using the random displacement scheme described by Banas et al. (2009b; see Visser 1997, North et al. 2006 for further discussion). The particle-tracking code, written in Java using the Processing toolkit (processing.org), is open-source, designed to work with any ROMS model, and available at *https://code.google.com/p/particulator/*.

The problem of keeping particles from becoming stranded on land through numerical errors is a universal one, and seldom dealt with systematically. We have taken a straightforward, safe approach: if a particular forward step is found to place a particle at a point with zero flow, that step is simply not applied. Thus no particles actually become stuck in land-masked areas in our calculation, but we cannot systematically prevent a few percent of the particles from becoming "nearly stuck": that is, asymptotically approaching an area of zero velocity, or becoming trapped in small, poorly resolved side channels for an unrealistically long time.

Furthermore, there is no obvious way to distinguish this numerical problem from the real phenomenon of trapping and long residence times in edge regions and secondary channels (Okubo 1973, Huzzey and Brubaker 1988, Ralston and Stacey 2005, Banas and Hickey 2005), and thus any attempt to filter the numerical issue from our age calculations would be arbitrary. The effect of this issue on our results is discussed below.

Each particle was associated with a particular volume of freshwater by taking daily streamflow timeseries for each river and dividing by the number of particles released per day (24). Since the rivers vary by several orders of magnitude in streamflow (Table 1), inventories of raw particle counts differ greatly from inventories of freshwater, as illustrated in Fig. 3 for a portion of Main Basin on a typical day in the middle of the 2006 simulation, Jun 5. Particles from all rivers are found intermingled in this region on this day (Fig. 3b), but when the particles are weighted by the freshwater volumes they represent, the largest rivers, the Fraser (purple) and Skagit (blue), clearly predominate.

The prime advantage of our particle-based approach over adding Eulerian passive tracers ("dye") to the ROMS model itself is that additional river-borne tracers, including nonconservative ones, can be represented entirely post-hoc simply by reweighting the single set of particle trajectories. To track distributions of freshwater, pathogens, and nutrients from 15 rivers would have required adding 45 passive tracers to each ROMS simulation year and thus many months of runtime on a computer cluster, whereas the entire particle analysis described here runs in a few days on a high-end laptop.

*Pathogen loading*

Fecal coliform concentrations were estimated as follows. Data from Washington Department of Ecology (DOE) sampling in the 14 Puget Sound rivers and Environment Canada sampling in the Fraser from 2000–present were used to define a lognormal distribution of concentrations for each month of the year for each river (Table 2). This distribution was then sampled randomly to associate each particle with a concentration and, using the particle's associated freshwater volume, an actual number of pathogens (colony forming units, cfu) carried by the particle at the time of its release. This statistical approach was taken because

measurements in the study years by themselves badly undersample event-scale variability in pathogen loadings. The data used to define monthly distributions were restricted to 2000–present because many of the rivers show significant trends in fecal coliform loads over several decades (Table 2). Note that no correlation was found between concentrations and flow volumes or loadings in the DOE dataset.

Mortality of fecal coliform in saltwater is high, and essential to include in a large-scale analysis. Mancini (1976) gives regressions for fecal coliform mortality as a function of temperature in fresh and saltwater. We applied a mortality rate of 0.8 $d^{-1}$ to all particles, corresponding to the mean temperature (11°C) in the surface 10 m from DOE monthly sampling at all Puget Sound stations in 2006. Seasonal variation in Puget Sound 0–10 m temperature (8–13°C) would suggest seasonal variation in fecal coliform mortality from 0.6–0.9 $d^{-1}$ according to the Mancini (1976) formula, but since scatter in the Mancini (1976) source data is well over a factor of two, this variation is not well-constrained and we have not included it or any further refinements.

*Nutrient loading*

An analogous method was used to associate the river particles with nutrient loads. Mohamedali et al. (2011) describes an estimation of dissolved inorganic nutrient (DIN) load over a typical annual cycle for each river. We applied monthly-mean DIN concentrations from that study (Table 3) to the particles and multiplied by their associated freshwater volumes to yield a DIN stock (mmol N) for each particle at the time of its release. Dissolved inorganic nitrogen does not, of course, remain dissolved or inorganic for long in nitrogen-limited but otherwise good growth conditions for phytoplankton, as found in Puget Sound over most of the spring and summer (Newton et al. 2002). Indeed, it is the uptake, settling out, and remineralization of river-contributed DIN that is of potential concern in Puget Sound, since this may contribute (alongside crucial ocean-driven processes) to hypoxia and acidification in some basins (Feely et al. 2010, Newton et al. 2011). Modeling the timescale of nutrient uptake and remineralization in detail would require a well-constrained biogeochemical model, beyond the scope of this analysis. Instead, here we use very simple assumptions regarding the export of DIN to make a very simple

point, that this process is fast compared with large-scale transport in Puget Sound and thus happens relatively close to each river source. We have modeled DIN as disappearing from the particle trajectories (through utilization by phytoplankton and vertical export) with a constant decay rate of $(6\ d)^{-1}$. This value was arrived at by assuming a plankton community in a 30 m euphotic zone with a pe- (export to production) ratio of 0.5 (Eppley and Peterson 1979, Dunne et al. 2005) and a detrital sinking rate of 10 m $s^{-1}$. The result also matches the decay time of total euphotic-zone nitrogen following a moderate phytoplankton bloom in the zero-dimensional coastal ecosystem model used for sensitivity studies by Banas et al. (2009a; see Table 2 in that study).

## Results

*Consistency check #1: volume flux*

Our Lagrangian reconstruction of Puget Sound circulation and freshwater distribution is noiser than, and potentially carries more numerical biases than, the Eulerian ROMS fields it is based on. Before proceeding with the analysis of individual river contributions, we will describe two consistency checks on the method overall. The first is based on the total volume fluxes represented by the particles, and the second is based on the total freshwater inventory and salinity deficit they represent.

We calculated overall connectivity and volume fluxes among five large subbasins of Puget Sound (Main Basin, South Sound, Hood Canal, Whidbey Basin, and Admiralty Inlet), in order to compare the total tidally-averaged volume flux by basin with previous estimates. Every 5 days throughout the 2005–2006 runs, particles were assigned to one of these five basins based on their mean position over a 25 hr tidal average, and the basin in which each particle was found after 20 d was also noted, yielding a time series of connectivity or transition matrices. This calculation ignores the previous history of the particles and their rivers of origin, or the fact that they were originally released in rivers at all, but it is still potentially biased by the anisotropic distribution of the particles in depth and plan view. To correct for this, particle counts were normalized by the volume of each basin in 10 m thick slabs. Results were aggregated into monthly averages, and the maximum and minimum of these are shown in Figure 4, expressed as

percentages of the volume of the basin of origin (black) and also as volume fluxes in $m^3\ s^{-1}$ (red).

Total volume fluxes through cross-sections at the seaward end of South Sound, Main Basin, Hood Canal, and Admiralty Inlet reconstructed by this method compare well with the total exchange flow (TEF) calculated by Sutherland et al. (2011), as shown in Table 2. This is an important verification that total transport in the ROMS model has for the most part been retained by the Lagrangian reconstruction. The one notable bias is the flux through the northern end of South Sound, i.e. the narrow, shallow sill of Tacoma Narrows. Either the intense tidal mixing that occurs at Tacoma Narrows or the large number of narrow, poorly resolved side channels in South Sound may be responsible for the bias in total volume flux. At the other three cross-sections where the geometry of the Sound allows a comparison with the Sutherland et al. (2011) TEF calculation, the bias is small, indicating that to first order, the particles are not dispersed overly fast or—a greater concern—retained artificially long by the particle-tracking numerics. This overall consistency check cannot, however, rule out the possibility that a small fraction of the particles are retained too long—perhaps, again, because of trapping in narrow or poorly resolved side channels—thus biasing age statistics more than volume-flux statistics.

*Consistency check #2: freshwater volume*

An attempt at reconstruction of the overall salinity field for several representative subbasins is shown in Fig. 5. Particle trajectories were sampled at 1 d intervals through 2005 and 2006 to create a timeseries of total freshwater volume in each basin, based on the hourly streamflow volume each particle was originally tagged with (see Methods). In Fig. 5b-f, these timeseries are shown as fractions of total basin volume, in aggregate and broken down by river of origin. In Fig. 5a, freshwater in Bellingham-Samish-Padilla Bays is shown subdivided into that carried by particles released in 2005 and that from 2006: the sum of these is what is shown in Fig. 5b. If the salinity $S_0$ of the marine (non-river) input to these basins does not vary and is known—both tenuous assumptions—then freshwater fraction $f$ can be converted into volume-mean salinity $(1 - f)\ S_0$. This reconstructed mean salinity is shown in Fig. 5g-k (dotted, red), with $S_0$ assumed, somewhat arbitrarily, to be 32 psu. Volume-mean salinity from ROMS (blue, solid) is also shown, along with depth-mean salinities (black dots) at stations monitored by the

Washington Department of Ecology.

Discrepancies between the three salinity time series (red, blue, black) are a conflation of several kinds of error and uncertainty: 1) single-point depth averages from observations vs. true volume averages from the model; 2) error in the ROMS hindcast, as discussed in detail by Sutherland et al. (2011); 3) numerical error in the particle-tracking calculation; 4) uncertainty and variation in $S_0$; and 5) a "hotstart/coldstart" issue that complicates the Eulerian-Lagrangian comparison for early 2006. The 2006 ROMS run was started not from the end of the 2005 run but rather from rest, using a nearest-neighbor interpolation from observations as its initial condition for salinity, whereas particles were in fact carried over from the 2005 run into 2006 (Fig. 5a). Thus at the beginning of 2006 there are salinity deficits in the domain that were never tagged by river particles (see, for example, the discontinuity at the start of 2006 in Fig. 5h). The persistence of this hotstart/coldstart discrepancy is potentially many months, comparable to the spinup discrepancies in the first part of 2005 (Fig. 5b-f, red vs. blue).

Despite these ambiguities, we can observe the following. In Bellingham-Samish-Padilla Bays, ROMS salinity and reconstructed salinity track very well throughout the 2006 seasonal cycle—a weak seasonal cycle, consisting mainly of an increase in salinity in mid-to-late summer—and also through a number of 1-3 week events (e.g., June and July). In Whidbey Basin, north Main Basin, and South Sound—as well as in the subbasins of Puget Sound not shown—the salinity reconstruction is biased high in early 2006 but converges with ROMS later in the year. In general, bias in the particle reconstruction is greatest where bias in salinity and temperature in the underlying ROMS model was found by Sutherland et al. (2011) to be greatest, e.g. South Sound and also southern Hood Canal (not shown). It is not obvious why these two kinds of bias should be spatially associated, but we speculate that the connection may be low horizontal resolution relative to channel width in areas with steep sidewalls.

Figure 5 is a stringest test of a technique (Lagrangian reconstruction of a complex salinity field) that has been rarely, if ever, attempted, let alone validated, and its overall success is only fair. Thus we proceed with the proviso that in early 2006, a first-order fraction of freshwater in inner Puget Sound may be unaccounted for by this analysis. Note, however, that this uncertainty decreases over the course of the simulation, and is much smaller in the seaward regions more

strongly forced, as we will show, by the large flows of the Fraser, Skagit, and Snohomish.

*Seasonal patterns of river influence*

As context for what follows, monthly means of surface salinity for 2006 are shown in Fig. 6. The seasonal cycle is complicated by the fact that Puget Sound's rivers do not share a single seasonal cycle of streamflow: low-altitude watersheds produce peak flows in winter, from rainfall, while higher-altitude watersheds have their peaks in early summer, through snowmelt. Some rivers thus have double-peaked seasonal cycles of streamflow (Table 1). The seasonal cycle of the regional winds—predominantly out of the south in winter and out of the north in summer (Halliwell and Allen 1984)—also affects freshwater distributions, most notably, the direction of the Fraser plume and its intrusion into the Strait of Juan de Fuca and Puget Sound (Fig. 6).

The fraction of Puget Sound freshwater originating in the two largest rivers, the Fraser and Skagit, is mapped in Fig. 7 by season. Here and below, three two-month averages are used to represent the seasonal cycle: Jan-Feb 2006 for winter, May-June for the spring freshet, Sep-Oct for the late summer low-flow period. Results are shown binned on a uniform 2 km grid, not the variable-resolution ROMS grid. The Fraser accounts for more than half the freshwater in the vicinity of the San Juan Islands year-round, and nearly half in Main Basin, South Sound, and northern Hood Canal in late summer. By late summer, the Skagit accounts for a further 1/3 of Main Basin freshwater. These results are the basis for our suggestion that Puget Sound be thought of as a kind of tributary estuary, at least for a portion of the year.

To highlight and differentiate the contributions of smaller rivers, in Fig. 8 we show the river contributing the largest freshwater fraction to each $(2\ \mathrm{km})^2$ bin in each season: color coding is as in Fig. 1. During winter, not just the Fraser and Skagit but seven other rivers are found to each dominate a particular province within our study area. The Skokomish is the largest freshwater contributor to most of Hood Canal. The Deschutes, Nisqually, and Puyallup partition South Sound and southern Main Basin, and Snohomish is the largest contributor to the northern half of Main Basin. The Nooksack and Samish both predominate in small regions near their mouths in Bellingham and Samish Bays. This pattern is an example of local river control, in the

sense that for most locations, the largest source of freshwater is the nearest major river. In contrast, in late summer (Fig. 8c), only northern Whidbey Basin is locally controlled in this sense: except for a few scattered locations, the Fraser is the largest freshwater contributor to almost all of Puget Sound and Bellingham-Samish-Padilla Bays. Spring (Fig. 8b) is intermediate between these local and nonlocal patterns.

The breakdown of these freshwater contributions by age (time since particle release at a river mouth) provides clues to the transport pathways that generate these patterns. Two contrasting examples are shown in Fig. 9. In Bellingham-Samish-Padilla Bays (Fig. 9a), the volume of Fraser water increases and the mean age of the Fraser fraction decreases starting early in summer, the time of the Fraser's annual peak and first sustained intrusion into the southern Salish Sea (Fig. 6). The smaller contributions of the Nooksack and Samish are younger, as one would expect for local as opposed to distant river inputs. In southern Hood Canal (Fig. 9b), which is more isolated and has a longer residence time, Fraser volume also increases in summer but with a longer delay after the early summer freshet. The contribution of the Skokomish and other local Hood Canal rivers (red) ages steadily from January to October before being suddenly flushed in the fall overturning (Newton et al. 2011).

Mean ages (Fig. 9) are in general longer than one would naively expect, given the basin-by-basin residence times of 20–140 d that previous studies have calculated (Babson et al. 2006, Paulson et al. 2006, Sutherland et al. 2011). This is true especially for the Fraser fraction. Almost all particle age distributions are strongly skewed (not shown), with a long tail indicating a small number of particles with very long ages (e.g. retention of 2005 particles in Fig. 5a). We suspect that this is in part a bias associated with a small number of "nearly stuck" particles, as discussed above.

*Sources of river-borne stressors*

Despite these caveats, the age distributions by river shown in Fig. 9 indicate a crucial general point: that different river fractions in one basin may have highly disparate ages, and thus age-dependent river-borne stressors may have very different distributions from freshwater as a whole. This conclusion is borne out for fecal coliform and DIN in Figs. 10–13.

Spatial distributions of statistically reconstructed fecal coliform loads were summed over the list of rivers. The *maximum* one-day-average concentration seen in each $(2\ \mathrm{km})^2$ bin in each two-month analysis window is shown in Fig. 10. As discussed above, each particle represents a certain number of colony forming units (cfu), a number that decays exponentially ($0.8\ \mathrm{d}^{-1}$) as the particle ages. These were summed in the vertical as well as on the 2 km grid; the result has units of cfu per area ($\mathrm{cfu\ (100\ ml)^{-1} \cdot m} = 10^4\ \mathrm{cfu\ m^{-2}}$) as opposed to the regulatory units of actual concentration ($\mathrm{cfu\ (100\ ml)^{-1}}$), and thus cannot be directly compared with Department of Health water-quality threshholds (Swanson 2008). Also, note that these integrated-concentration maps (Fig. 10) represent only the contributions from major rivers, and may be very different from total load from all sources. For example, urban runoff directly into Puget Sound is not included (nor is it well measured). The purpose of this calculation is solely to provide context for the ranking of major-river fecal coliform sources (Fig. 11). Areas with maximum integrated concentration below the lower end of the color scale used in Fig. 10 ($3\ \mathrm{cfu\ (100\ ml)^{-1}\ m}$, which corresponds to 6–12 $\mathrm{cfu\ (100\ ml)^{-1}}$ in a hypothetical nearshore area of depth 2–4 m) are considered not to be influenced by any major river, and are shown as gray in Fig. 11.

In winter (Fig. 11a), the map of dominant fecal coliform contributor is similar to the map of dominant freshwater contributors (Fig. 8a), with each of 8 rivers dominating over an area of 10–100 km near its outlet. The principal differences are that the Nooksack and Duwamish are more significant contributors of fecal coliform than freshwater, in relative terms, and that large areas of Hood Canal, Admiralty Inlet, and the Strait of Juan de Fuca effectively receive no major-river fecal coliform contribution at all. In Puget Sound in spring and summer (Fig. 11b,c), the fecal coliform contributor maps are very similar to the winter map, and thus very different from the freshwater contributor maps from those seasons, which are highly dominated by the Fraser. In Bellingham and Samish Bays, it appears that the Fraser may be as significant a source of fecal coliform as the local rivers, the Nooksack and Samish.

Results are similar for DIN. Total load from the major rivers is shown in Fig. 12, subject to the $(6\ \mathrm{d})^{-1}$ decay rate representing export from the euphotic zone discussed above. Concentrations are, as in Fig. 11, vertically integrated, in $\mathrm{mmol\ m^{-2}}$, not $\mathrm{mmol\ m^{-3}}$. Note also that marine-derived nitrate dominates the nitrogen budget of Puget Sound (Newton et al. 2002,

Paulson et al. 2006, Steinberg et al. 2010, Mohamedali et al. 2011), and so this map is an indicator of river influence but not overall nutrient status or hypoxia risk. Here, as for fecal coliform, areas below a minimum integrated concentration (1 mmol $m^{-2}$) are shown as gray in the map of dominant DIN contributors (Fig. 13). Patterns of DIN contributors by season (Fig. 12) are similar to the fecal coliform maps: that is, in winter similar to the freshwater contributor map (Fig. 8a) and in spring and summer very different from the freshwater pattern, with much less Fraser influence and much more local-river dominance.

**Discussion**

We have shown that river-borne tracers with long and short lifespans in saltwater have very different patterns of seasonal distribution in Puget Sound and the central Salish Sea. Fig. 14 provides a summary, quantitative statement of this conclusion, maps of mean distance to river of origin for freshwater, fecal coliform, and DIN, in late spring/early summer. Fecal coliform and DIN in most of Puget Sound, including Main Basin, are predominantly local (10–50 km), while freshwater is not.

This analysis only concerns the contributions of major rivers, however, and this is very different from a comprehensive mapping of pathogens and nutrients. In Table 4, we have attempted to situate our results within a fuller overview of factors affecting Puget Sound nearshore areas. For concreteness we have focused this overview on shellfish health and productivity, a "keystone" environmental concern that unites many others.

Nutrient loading affects Puget Sound shellfish growing areas not only through the threat of hypoxia, as we have emphasized in our framing, but also by fueling productivity. A companion study (Conway-Cranos et al, in preparation) has shown that particulate organic matter from nearby salt marshes is an important component of oyster diet in both central Hood Canal and Samish Bay. DIN from major rivers, as this study has considered, is most likely to contribute to shellfish diet on somewhat larger scales, by contributing fractionally to marine diatom production. This watershed contribution must be understood in the context of the fact that most of the nutrients in Puget Sound arrive from the ocean by natural processes (Mackas and Harrison 1997, Mohamedali et al. 2011). Puget Sound is, like other Pacific Northwest estuaries

(Hickey and Banas 2003), a tributary to a major upwelling zone, and its nutrient and oxygen budgets are strongly forced by variability in the oceanic sourcewater and physical dynamics at the entrance sills that control the intrusion of this sourcewater (Cannon et al. 1990, Masson 2002, Babson et al. 2006, Newton et al. 2011). Thus beyond the "remote" influence of the Fraser is the even larger and more remote influence of the coastal ocean. Note that particularly during winter, ocean influences on the Salish Sea include intrusions of the Columbia River plume, previously described as the "Olympic Peninsula Countercurrent" in the Strait of Juan de Fuca (Thomson et al. 2007).

For pathogen loading, the elephant in the room (Table 4) is non-point-source runoff from urban areas, which we have not modeled and which is not systematically monitored. Regulatory agencies have tended to presume that nearshore areas receiving direct urban runoff are not safe for aquaculture or shellfish harvest and invest their monitoring resources in areas of greater uncertainty. Thus to produce an analog to Fig. 10 that shows total fecal coliform concentrations or risk, as opposed to the major-river fraction only, is as much an empirical problem as a modeling task.

Perhaps the most provocative result from this study is the indication that the Fraser River may be contributing a overall pathogen load to Samish Bay comparable to that from the local river, the subject of much recent regulatory attention (Swanson et al. 2008, Lawrence et al. 2009). The circulation model used here is unable to pursue this idea down to the scale of the intertidal areas where shellfish are grown in Samish Bay. One would also need to focus a model analysis of the problem down in time, to individual weather events—combinations of wind and riverflow—to assess the hazard posed by remote as opposed to local sources of bacterial pollution. On longer timescales, both the Fraser and Samish, like almost all the watersheds surveyed, show downward trends in fecal coliform loads over several decades (Fig. 2). Since the trends in the local and distant rivers are in the same direction, it is not obvious whether the balance of local and remote sources of pathogens—in Samish Bay or elsewhere—could be expected to change in coming decades.

**Conclusion**

To our knowledge this is the first attempt to account for the entire freshwater content of a complex estuarine system in a Lagrangian frame. Methodologically speaking, the results of this experiment are promising but also highlight numerical limitations that otherwise might well escape notice, if, as is far more common, we were simply attempting to track some representative patches of freshwater in the model rather than all of it. The reconstruction of volume-mean salinity over time from ~200,000 particles is quite good in Bellingham-Samish-Padilla Bays (Fig. 5g) and grows progressively worse (Fig. 5h-k, red vs blue lines) as one progresses landward: intriguingly, this pattern of error between the Lagrangian and Eulerian versions of the model fields matches the pattern of error between the Eulerian base model and field observations. We suspect that any modern, practical particle-tracking scheme would show a similar slow degradation in accuracy, if used to track particles for hundreds of days in strong tidal flow in narrow, steep topography. We hope that the combination of 1) fair-to-good success of the salinity reconstruction, 2) ability of this technique to address connectivity and water-age questions that observations cannot, and 3) extremely low computational cost inspire similar efforts in other systems, and further work on the numerical issues involved.

Much applied marine research in Puget Sound has appeared to be guided by the implicit hypothesis that river influences on water quality at a given site reflect the impact of the nearest major river. For the two water-quality problems we examined—pathogen and DIN loading—this proves to be a good rule of thumb for most of Puget Sound, throughout the seasonal cycle. However, it also appears that for freshwater itself and long-lived river-borne tracers, this rule of thumb could be quite misleading in spring and summer. Except in winter, when streamflow from lowland watersheds is strong and the prevailing winds keep the Fraser plume in the Strait of Georgia, our model suggests that the Fraser is the largest single source of freshwater to Main Basin and many other reaches of Puget Sound, followed by the large rivers of Whidbey Basin. The Fraser's influence is particularly strong in the central Salish Sea—the San Juan Islands and Bellingham-Samish-Padilla Bays—where in fact it appears possible (no stronger statement can be made using the existing circulation model) that the Fraser is contributing to fecal-coliform contamination in Samish Bay.

The difference in connectivity patterns between river water itself and important river-borne stressors leads to the conclusion that local salinity cannot be used as a reliable indicator of the influence of local rivers on water quality, even to a first approximation, except perhaps within a few km of a river mouth. A hybrid approach that combines salinity and water-quality monitoring with well-validated, high-resolution models holds greater promise.

**Acknowledgements**

This study was partly funded by EPA Grant DW-13-92327601-01.

Babson, A. L., M. Kawase, and P. MacCready, 2006: Seasonal and interannual variability in the circulation of Puget Sound, Washington: A box model study. Atmos.–Ocean, 44, 29–45.

Banas NS, Lessard EJ, Kudela RM, MacCready P, Peterson TD, Hickey BM, Frame E (2009a) Planktonic growth and grazing in the Columbia River plume region: A biophysical model study. J Geophys Res 114:C00B06.

Banas NS, MacCready P, Hickey BM (2009b) The Columbia River plume as cross-shelf exporter and along-shelf barrier. *Cont. Shelf Res.*, 29:292-301.

Banas, N. S., and B. M. Hickey, 2005: Mapping exchange and residence time in a model of Willapa Bay, Washington, a branching, macrotidal estuary. J. Geophys. Res., 110, C11011, doi:10.1029/2005JC002950.

Barron, C. N., A. B. Kara, P. J. Martin, R. C. Rhodes, and L. F. Smedstad, 2006: Formulation, implementation and examina- tion of vertical coordinate choices in the global Navy Coastal Ocean Model (NCOM). Ocean Modell., 11, 347–375.

Barron, C.N., L. F. Smedstad, J. M. Dastugue, and O. M. Smedstad, 2007: Evaluation of ocean models using observed and simulated drifter trajectories: Impact of sea surface height on synthetic profiles for data assimilation. J. Geophys. Res., 112, C07019, doi:10.1029/2006JC003982.

Cannon, G A, J R Holbrook, and D J Pashinski. 1990. Variations in the Onset of Bottom-Water Intrusions Over the Entrance Sill of a Fjord. *Estuaries and Coasts* 13 (1): 31–42.

Cuo, Lan, Tazebe K Beyene, Nathalie Voisin, Fengge Su, Dennis P Lettenmaier, Marina Alberti, and Jeffrey E Richey. 2011. Effects of Mid-Twenty-First Century Climate and Land Cover Change on the Hydrology of the Puget Sound Basin, Washington. *Hydrological Processes* 25 (11) (January 1): 1729–1753. doi:10.1002/hyp.7932.

Dunne, John P, Robert A Armstrong, Anand Gnanadesikan, and Jorge L Sarmiento. 2005. Empirical and Mechanistic Models for the Particle Export Ratio. *Global Biogeochemical Cycles* 19 (4): GB4026. doi:10.1029/2004GB002390.

Eppley, Richard W, and Bruce J Peterson. 1979. “Particulate Organic Matter Flux and Planktonic New Production in the Deep Ocean.” *Nature* 282: 677–680.

Feely, R A, S R Alin, J Newton, and C L Sabine. 2010. “The Combined Effects of Ocean Acidification, Mixing, and Respiration on pH and Carbonate Saturation in an Urbanized

Estuary." *Estuarine*, *Coastal and Shelf Sci* 88:442-449.

Halliwell, G R, and J S Allen. 1984. "Large-Scale Sea Level Response to Atmospheric Forcing Along the West Coast of North America, Summer 1973." *J Phys Oceanogr 14:862-886*.

Hickey, B M, and Neil S Banas. 2003. "Oceanography of the US Pacific Northwest Coastal Ocean and Estuaries with Application to Coastal Ecology." *Estuaries and Coasts* 26:1010-1031.

King County (2000) Habitat-limiting factors and reconnaissance assessment report. Green/Duwamish and Central Puget Sound Watersheds (Water Resource Inventory Area 9 and Vashon Island). Prepared by King County Department of Natural Resources, Seattle, WA and Washington State Conservation Commission, Olympia, WA

Lawrence, Sally. 2009. *Samish Bay Watershed Fecal Coliform Bacteria TMDL - Volume 2: Water Quality Implementation Plan*. Washington State Department of Ecology.

Mackas, David L, and Paul J Harrison. 1997. Nitrogenous Nutrient Sources and Sinks in the Juan De Fuca Strait/Strait of Georgia/Puget Sound Estuarine System: Assessing the Potential for Eutrophication. *Estuarine, Coastal and Shelf Science* 44 (1): 1–21.

Mancini, J L. 1978. "Numerical Estimates of Coliform Mortality Rates Under Various Conditions." *Journal of the Water Pollution Control Federation* 50:2477–2484.

Mass, C. F., and Coauthors, 2003: Regional environmental prediction over the Pacific Northwest. Bull. Amer. Meteor. Soc., 84, 1353–1366.

Masson D (2002) Deep Water Renewal in the Strait of Georgia. *Estuarine, Coastal and Shelf Science* 54:115–126.

Mohamedali, T M, Mindy Roberts, Brandon Sackmann, and Andrew Kolosseus. 2011. *Puget Sound Dissolved Oxygen Model Nutrient Load Summary for 1999-2008*. Washington State Department of Ecology. http://www.ecy.wa.gov/biblio/1103057.html.

North EW, Hood RR, Chao SY, Sanford LP (2006) Using a random displacement model to simulate turbulent particle motion in a baroclinic frontal zone: A new implementation scheme and model performance tests. *Journal of Marine Systems* 60:365–380.

Newton, J.A., S.L. Albertson, K. Van Voorhis, C. Maloy, and E. Siegel (2002) *Washington State Marine Water Quality, 1998 through 2000.* Washington State Department of Ecology, Environmental Assessment Program, Publication #02-03-056, Olympia, WA.

Newton JA, Bassin CJ, Devol A, Richey J, Kawase M, Warner J (2011) Hood Canal Dissolved Oxygen Program Integrated Assessment and Modeling Report, Chapter 1, Overview and Results Synthesis. *http://www.hoodcanal.washington.edu/news-docs/publications.jsp.*

Paulson, A.J., Konrad, C.P., Frans, L.M., Noble, M.A., Kendall, Carol, Josberger, E.G., Huffman, R.L., and T.D. Olsen. 2006. Freshwater and Saline Loads of Dissolved Inorganic Nitrogen to Hood Canal and Lynch Cove, Western Washington. U.S. Geological Survey Scientific Investigations Report, 2006-5106, 91 p.

Ralston DK, Stacey MT (2005) Longitudinal dispersion and lateral circulation in the intertidal zone. *J Geophys Res* 110:C07015.

Pritchard, D. W., and R. E. Bunce, 1959: Physical and chemical hydrography of the Magothy River. Chesapeake Bay Institute Tech. Rep. XVII, Ref. 59–2.

Pritchard, D. W., and J. H. Carpenter, 1960: Measurements of turbulent diffusion in estuarine and inshore waters. *Bull. Int. Assoc. Sci. Hydrol.,* **20,** 37–50.

Rocchini, R J, W A Bergerud, and R W Drinnan. 1981. *Fraser River Estuary Study, Water Quality, Survey of Fecal Coliforms in 1978*. Province of British Columbia, Ministry of Environment, Assessment and Planning Division.

Schroeder, W. W., S. P. Dinnel, and W. J. Wiseman Jr., 1992: Salinity structure of a shallow, tributary estuary. *Dynamics and Exchanges in the Coastal Zone,* D. Prandle, Ed., Amer. Geophys. Union, 155–171.

Steinberg PD, Brett MT, Bechtold JS, Richey JE, Porensky LM, Smith SN (2010) The influence of watershed characteristics on nitrogen export to and marine fate in Hood Canal, Washington, USA. *Biogeochemistry* 106:415–433.

Sutherland DA, MacCready P, Banas NS, Smedstad LF (2011) A numerical modeling study of what controls the salt content and total exchange flow in the Salish Sea. *J. Phys. Oceanogr.*, 41:1125-1143, doi:10.1175/2011JPO4540.

Swanson T (2008) Samish Bay Fecal Coliform Bacteria Total Maximum Daily Load: Volume 1,

Water Quality Study Findings. Washington Department of Ecology, #08-03-029. 131 pp.

Thomson RE, Mihály SF, Kulikov EA (2007) Estuarine versus transient flow regimes in Juan de Fuca Strait. *J Geophys Res* 112:C09022.

Wolk, Frank. 2003. Three-Dimensional Lagrangian Tracer Modelling in Wadden Sea Areas. Diploma thesis, Carl von Ossietzky University Oldenburg. 80 pp.

| | watershed area[a] ($km^2$) | percentage of watershed above 1000 m[a] (%) | Mean flow, 2006[c] ($m^3\ s^{-1}$) | | | |
|---|---|---|---|---|---|---|
| | | | annual | Jan–Feb | May–June | Sep–Oct |
| *Puget Sound* | | | | | | |
| Skagit | 8316 | 72 | 471 | 684 | 593 | 148 |
| Snohomish | 4430 | 35 | 288 | 459 | 371 | 71 |
| Puyallup | 2613 | 40 | 107 | 165 | 127 | 37 |
| Nisqually | 1955 | 17 | 47 | 105 | 29 | 14 |
| Stillaguamish | 1722 | 15 | 59 | 112 | 55 | 10 |
| Duwamish/Green | 1466[b] | n/d | 46 | 94 | 33 | 9 |
| Skokomish | 620 | 27 | 52 | 134 | 18 | 5 |
| Cedar | 469 | 21 | 31 | 69 | 22 | 9 |
| Deschutes | 435 | 1 | 10 | 22 | 3 | 1 |
| Dosewallips | 301 | 62 | 15 | 24 | 21 | 2 |
| Hamma Hamma | 216 | 44 | 15 | 24 | 21 | 2 |
| Duckabush | 197 | 57 | 15 | 24 | 21 | 2 |
| | | | | | | |
| *central Salish Sea* | | | | | | |
| Nooksack | | | 115 | 185 | 148 | 28 |
| Samish | | | 7 | 17 | 3 | 1 |
| Fraser | | | 2184 | 1205 | 5201 | 1143 |

*Table 1. Watershed characteristics and streamflow statistics for the 15 major rivers included in this study. Data are taken from [a]Cuo et al. (2011); [b]King County (2000); [c]Sutherland et al. (2011).*

| | Total exchange flow (TEF) through seaward end (Sutherland et al. 2011), annual average, $10^3$ m$^3$ s$^{-1}$ | Volume flux reconstructed from 20 d particle trajectories (this study), annual mean ± std dev, $10^3$ m$^3$ s$^{-1}$ |
|---|---|---|
| South Sound | 7.6 | 5.1 ± 0.6 |
| Main Basin | 20 | 21 ± 3 |
| Hood Canal | 3.1 | 3.9 ± 0.8 |
| Admiralty Inlet | 29 | 26 ± 3 |

*Table 2. Comparison of Eulerian and Lagrangian model estimates of volume fluxes through several subbasins of Puget Sound.*

| | 2000–present | | | 1970–1985 |
|---|---|---|---|---|
| | 10%ile | median | 90%ile | 90%ile |
| *Puget Sound* | | | | |
| Skagit | 1 | 5 | 30 | 98 |
| Snohomish | 5 | 17 | 66 | 320 |
| Puyallup | 9 | 39 | 130 | 600 |
| Nisqually | 1 | 9 | 23 | 88 |
| Stillaguamish | 2 | 13 | 110 | 260 |
| Duwamish/Green | 8 | 30 | 210 | — |
| Skokomish | 1 | 6 | 26 | 17 |
| Cedar | 3 | 37 | 140 | 180 |
| Deschutes | 4 | 25 | 69 | 100 |
| Duckabush | 1 | 2 | 9 | — |
| *North of Puget Sound* | | | | |
| Nooksack | 9 | 26 | 90 | 460 |
| Samish | 12 | 44 | 280 | 360 |
| Fraser | 15 | 51 | 640 | 3320 |

*Table 3. Annual statistics of fecal coliform concentrations, in cfu (100 ml)$^{-1}$, for major rivers included in this study. Data from WA Department of Ecology for all rivers except the Fraser. Fraser data from Environment Canada Gravesend buoy, station BC08MH0453, 2008–2012, and three sites in the lower Fraser in 1978 as reported by Rocchini et al. (1981). For 2000–present, n > 120 for all stations except the Fraser (n=47). For 1970–1985, n > 100 except Skagit (n=63) and Skokomish (n=26). Doeswallips and Hamma Hamma (Table 1) were not monitored.*

| | *Total nutrients* | *Fecal coliform* | *Freshwater, long-lived tracers* |
|---|---|---|---|
| 100 m – 1 km | salt marshes | urban runoff | — |
| 1 – 10 km | direct contribution of local river | direct contribution of local river | tidal and event-scale influence of local river |
| 10 – 50 km | weak influence of nearby rivers | weak influence of nearby rivers | local river (winter) |
| > 100 km | ocean inputs | Fraser River (in Bellingham Bay, Samish Bay, San Juan Islands) | distant, major rivers (Fraser, Skagit, all seasons but esp. summer; Columbia, winter–spring) |

*Table 4. Summary of spatially nested influences on nearshore water quality and trophic subsidies in Puget Sound and central Salish Sea waters.*

Figure 1. *(a)* Map of Puget Sound and surrounding waters of the Salish Sea, with *(b,c)* enlargements of the northern and southern portions of the study domain. Colored dots mark the mouths of the 15 rivers considered in this study, where particles were released in the circulation model.

Figure 2. Annual cycle of riverflow for the Fraser River and the 14 Puget Sound/central Salish Sea rivers shown in Fig. 1b,c, for 2005 (dashed lines) and 2006 (solid lines).

Figure 3. Instantaneous position of all particles released in the 2006 model run on Jun 5, 2006. Particles are color-coded by river as in Fig. 1. Approximately 1% of particles are visible. *(a)* The entire model domain is shown in *(a)* and a $(25\ \mathrm{km})^2$ area of central Main Basin in *(b,c)*. In *(a,b)*, particles are all equally weighted, each representing one hour of flow from one river; in *(c)*, they are weighted by the freshwater volume entering Puget Sound in that hour, and in this weighting, the largest rivers, most notably the Fraser (purple), predominate.

Figure 4. Overall connectivity among five subbasins of Puget Sound. Percentages of the volume of each subbasin transported to each other subbasin over 20 d are shown in black; the same transports converted to volume flux in $\mathrm{m^3\ s^{-1}}$ are shown in red. Ranges show the maximum and minimum among monthly-mean transports for the 24 months of 2005 and 2006. Transports below 200 $\mathrm{m^3\ s^{-1}}$ are omitted for clarity; transports below 800 $\mathrm{m^3\ s^{-1}}$ are grayed and dashed. Arrows pointing outward (not toward a subbasin) represent the volume fraction found outside Puget Sound after 20 d. Note that these particles exit primarily via Admiralty Inlet (a smaller fraction exits directly from Whidbey Basin, via Deception Pass) and that the arrows pointing to Admiralty Inlet represent water parcels that end in it, not particles that pass through it.

Figure 5. Timeseries of freshwater fraction and mean salinity for five subregions *(b-f)*, reconstructed from inventories of particles. Stacked area plots show the breakdown of freshwater volume by river of origin over two simulation years: color-coding is as in Fig. 1, and major river contributions are labeled by name. The contributions of particles released in 2005 and in 2006 are shown separately in *(a)* for the Bellingham-Samish-Padilla Bay system. *(g-k)* Line plots show volume-mean salinity from ROMS (blue, solid) in comparison with the particle-based reconstruction (red, dotted). Instantaneous depth-mean salinity from CTD casts within each subregion are also shown (black dots).

Figure 6. Monthly averages of surface salinity in the Sutherland et al. (2011) model for 2006.

Figure 7. Fraction of total freshwater that originated in *(a,b,c)* the Fraser River and *(d,e,f)* the Skagit, averaged over two-month periods: *(a,d)* Jan-Feb 2006, *(b,e)* May-June 2006, and *(c,f)* Sep-Oct 2006. Results are shown not on the ROMS model grid, but regridded at 2 km resolution.

Figure 8. River contributing the largest fraction of total freshwater to each point in Puget Sound, in three two-month averages (winter, late spring/early summer, late summer) as in Fig. 7. Results are gridded at 2 km resolution. Rivers are color-coded as in Fig. 1, and major contributors are labeled by name.

Figure 9. Mean age of the freshwater contribution from each river to two subregions, (a) the Bellingham-Samish-Padilla Bay system and (b) South Hood Canal, over a seasonal cycle. Dots are color-coded by river as in Fig. 1 and sized according to freshwater volume.

Figure 10. Fecal coliform load to Puget Sound originating in the 15 major rivers included in this study, in three seasons, *(a)* winter, *(b)* late spring/early summer, *(c)* late summer. For each season the maximum daily pathogen count is shown, vertically integrated (colony forming units per unit area, not per unit volume).

Figure 11. River contributing the largest fraction of fecal coliform, gridded at 2 km resolution, in three seasons: compare Fig. 8. Areas with maximum daily concentration < 3 cfu $(100\ \mathrm{ml})^{-1}$ m (the low end of the scale in Fig. 10) are grayed.

Figure 12. Mean distribution of dissolved inorganic nitrogen supplied by the 15 major rivers included in this study, averaged over three seasons. Note that concentrations are vertically integrated (mmol N per unit area, not per unit volume).

Figure 13. River contributing the largest fraction of DIN, gridded at 2 km resolution, in three seasons: compare Figs. 8, 11. Areas with integrated mean concentration < 1 mmol $\mathrm{m}^{-2}$ (the low end of the scale in Fig. 12) are grayed.

Figure 14. Mean distance to river of origin in spring/early summer, for freshwater (compare Fig. 8b), fecal coliform (compare Fig. 11b), and DIN (compare Fig. 13b).

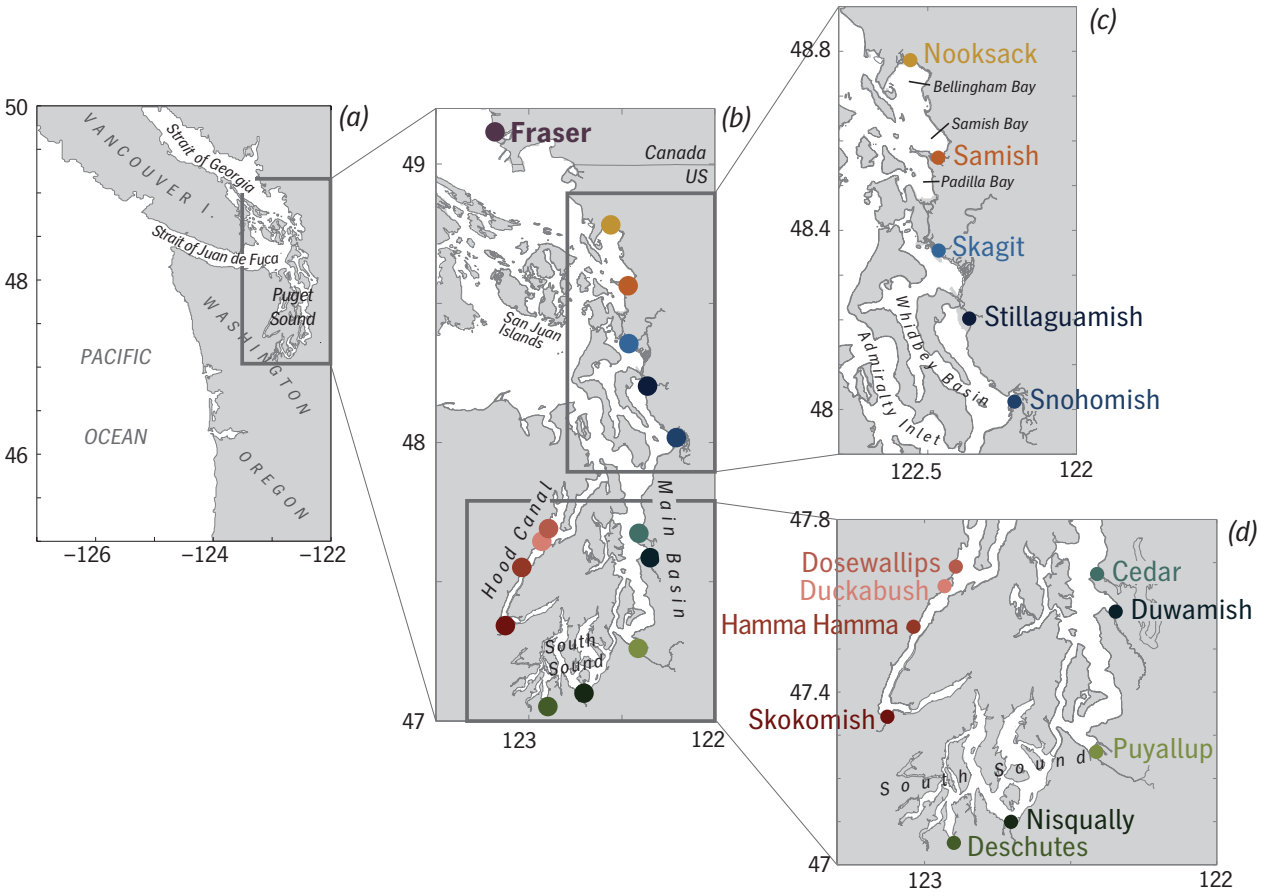


Figure 1. (a) Map of Puget Sound and surrounding waters of the Salish Sea, with (b,c) enlargements of the northern and southern portions of the study domain. Colored dots mark the mouths of the 15 rivers considered in this study, where particles were released in the circulation model.

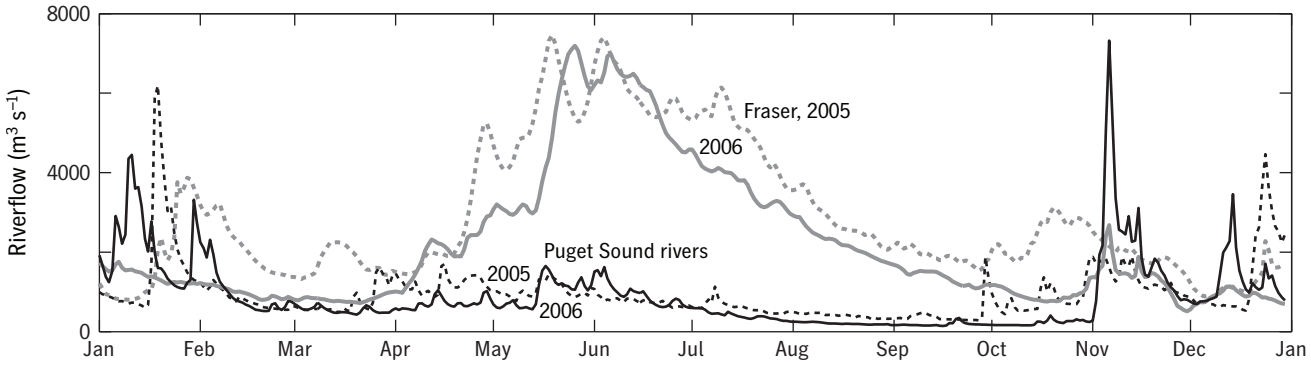


Figure 2. Annual cycle of riverflow for the Fraser River and the 14 Puget Sound/central Salish Sea rivers shown in Fig. 1b,c, for 2005 (dashed lines) and 2006 (solid lines).

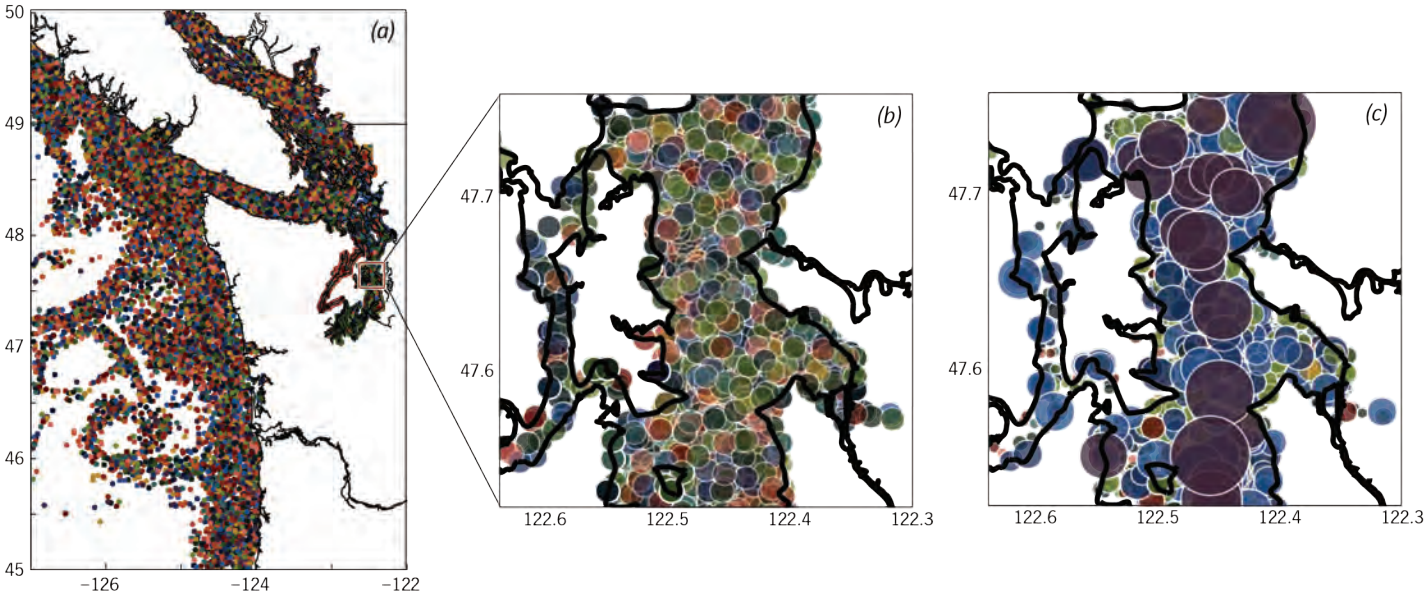


Figure 3. Instantaneous position of all particles released in the 2006 model run on Jun 5, 2006. Particles are color-coded by river as in Fig. 1. Approximately 1% of particles are visible. (a) The entire model domain is shown in (a) and a (25 km)2 area of central Main Basin in (b,c). In (a,b), particles are all equally weighted, each representing one hour of flow from one river; in (c), they are weighted by the freshwater volume entering Puget Sound in that hour, and in this weighting, the largest rivers, most notably the Fraser (purple), predominate.

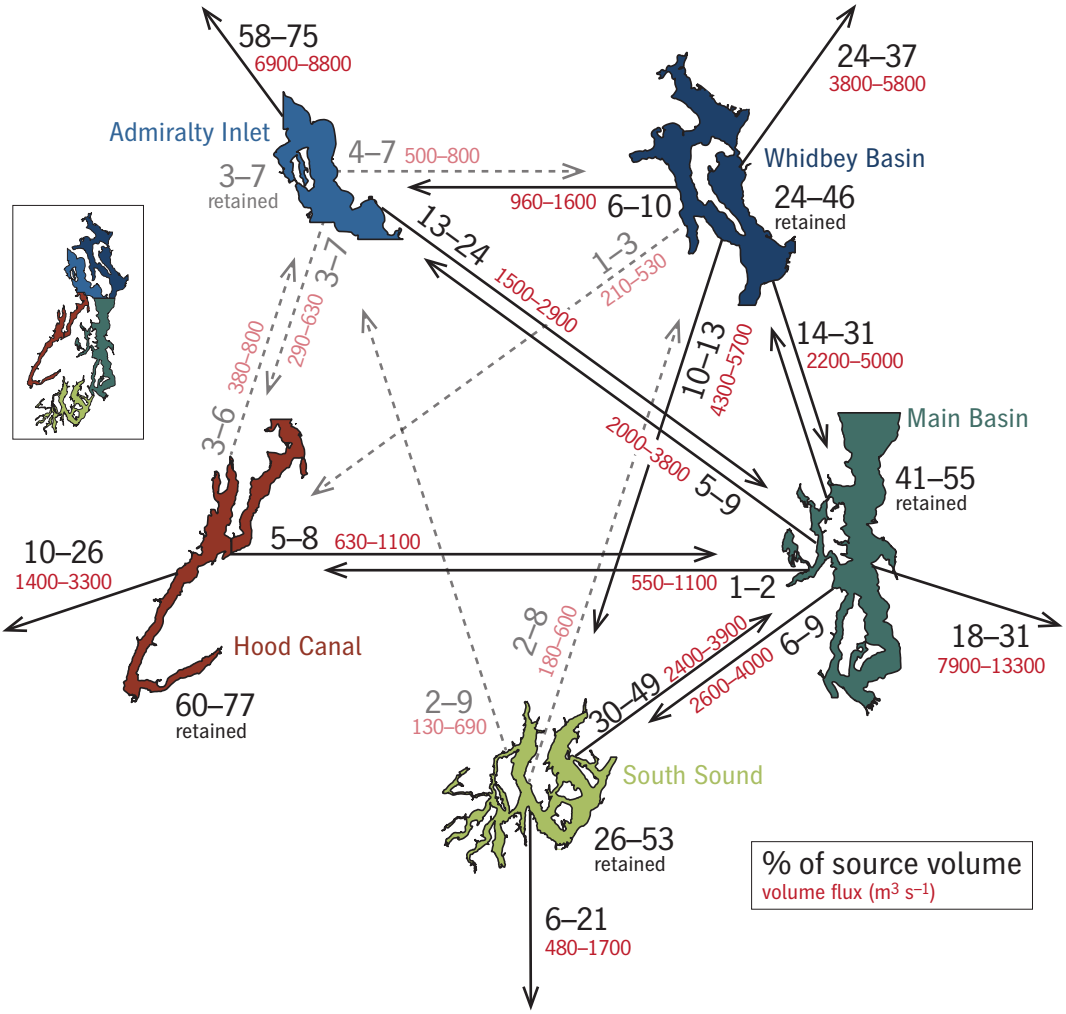


Figure 4. Overall connectivity among five subbasins of Puget Sound. Percentages of the volume of each subbasin transported to each other subbasin over 20 d are shown in black; the same transports converted to volume flux in m3 s–1 are shown in red. Ranges show the maximum and minimum among monthly-mean transports for the 24 months of 2005 and 2006. Transports below 200 m3 s–1 are omitted for clarity; transports below 800 m3 s–1 are grayed and dashed. Arrows pointing outward (not toward a subbasin) represent the volume fraction found outside Puget Sound after 20 d. Note that these particles exit primarily via Admiralty Inlet (a smaller fraction exits directly from Whidbey Basin, via Deception Pass) and that the arrows pointing to Admiralty Inlet represent water parcels that end in it, not particles that pass through it.

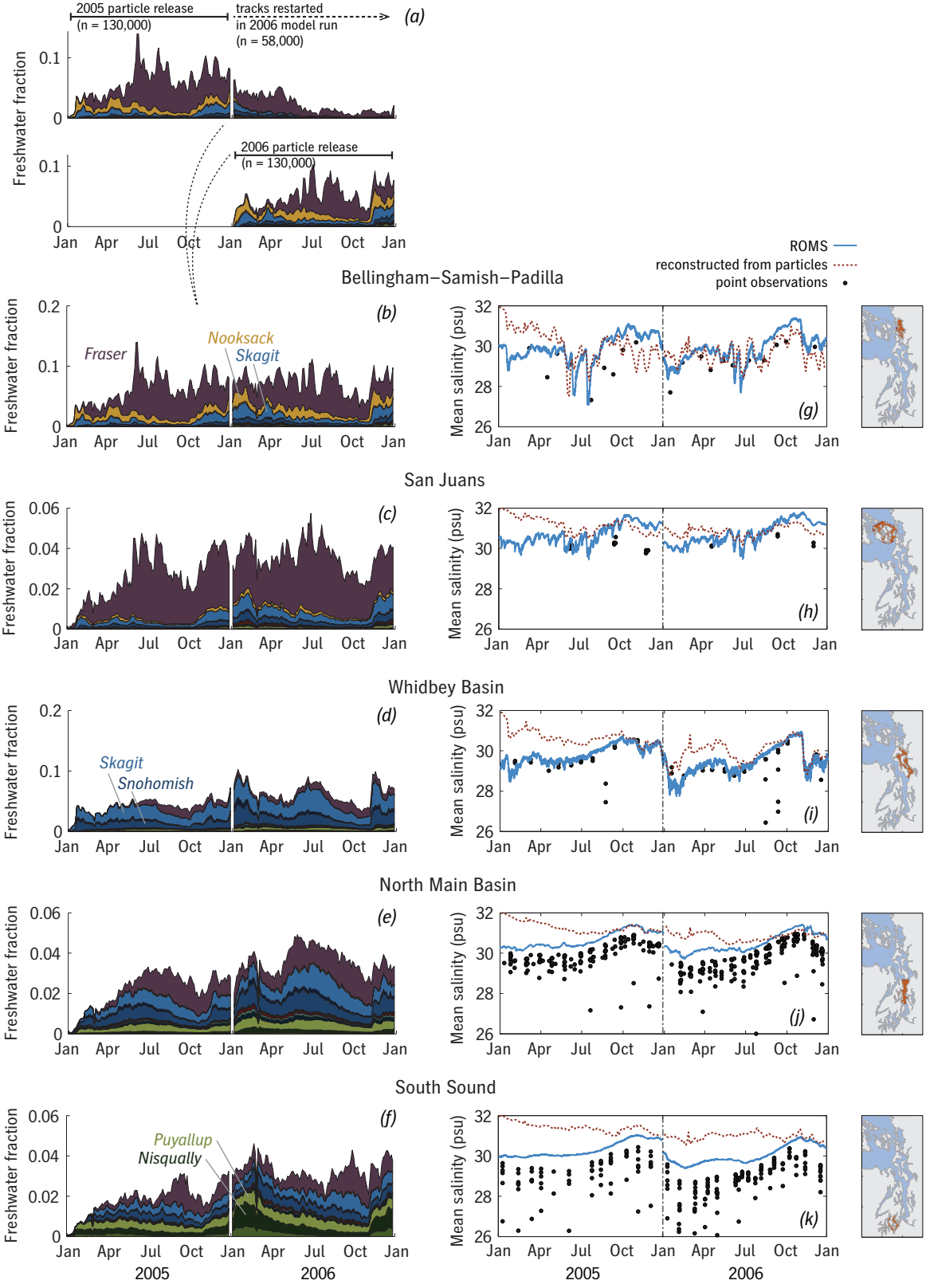


Figure 5. Timeseries of freshwater fraction and mean salinity for five subregions (b-f), reconstructed from inventories of particles. Stacked area plots show the breakdown of freshwater volume by river of origin over two simulation years: color-coding is as in Fig. 1, and major river contributions are labeled by name. The contributions of particles released in 2005 and in 2006 are shown separately in (a) for the Bellingham-Samish-Padilla Bay system. (g-k) Line plots show volume-mean salinity from ROMS (blue, solid) in comparison with the particle-based reconstruction (red, dotted). Instantaneous depth-mean salinity from CTD casts within each subregion are also shown (black dots).

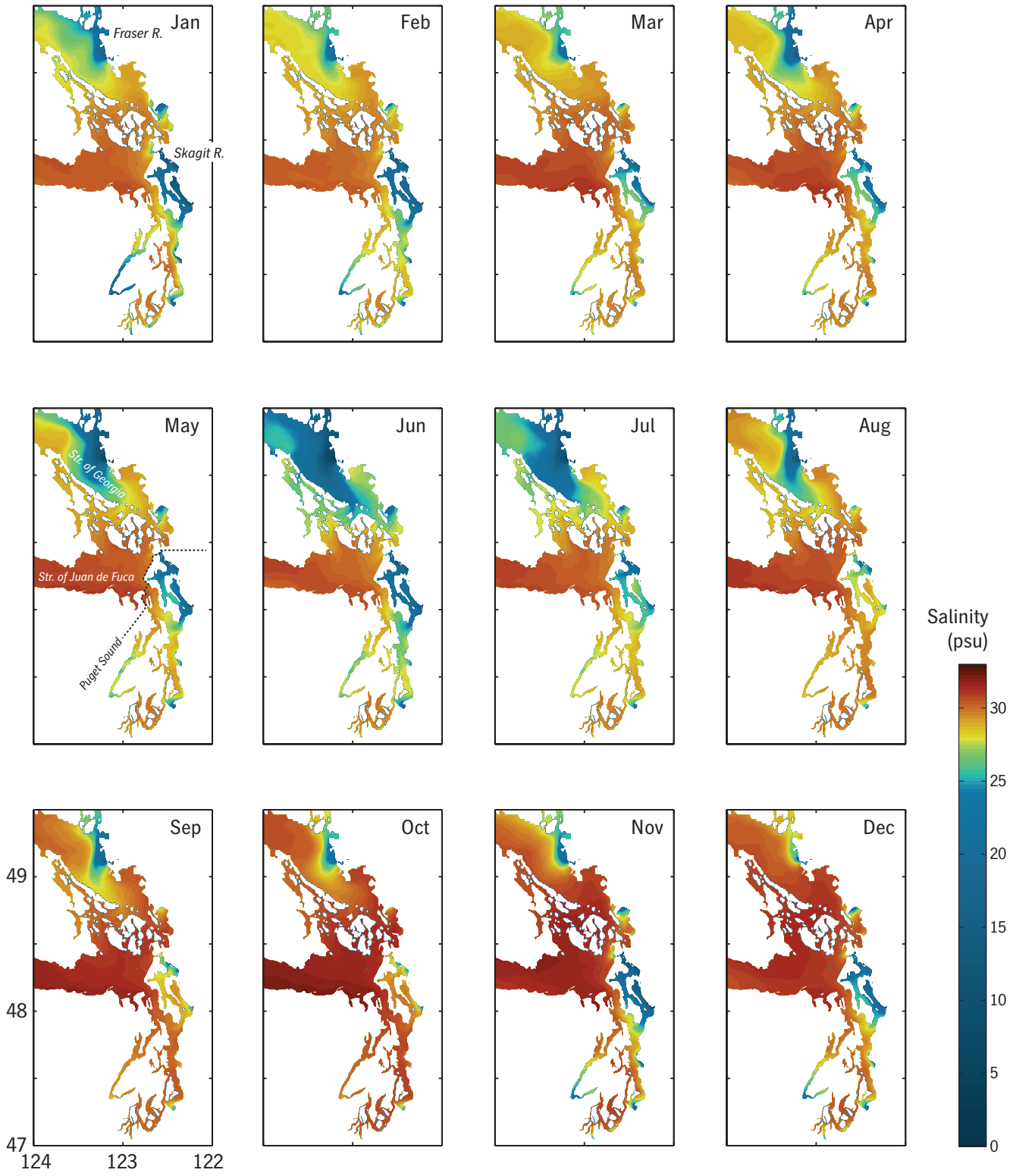


Figure 6. Monthly averages of surface salinity in the Sutherland et al. (2011) model for 2006.

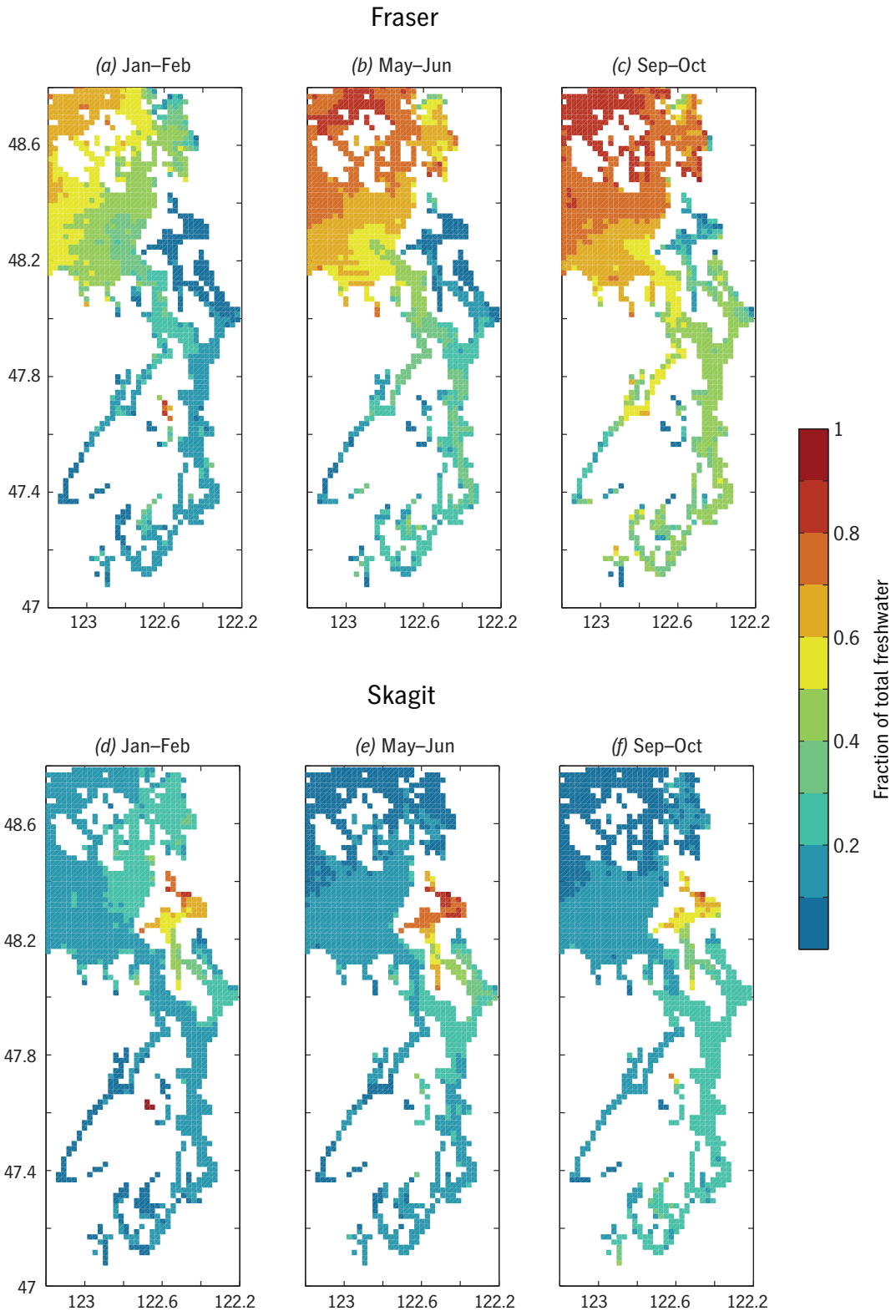


Figure 7. Fraction of total freshwater that originated in (a,b,c) the Fraser River and (d,e,f) the Skagit, averaged over two-month periods: (a,d) Jan-Feb 2006, (b,e) May-June 2006, and (c,f) Sep-Oct 2006. Results are shown not on the ROMS model grid, but regridded at 2 km resolution.

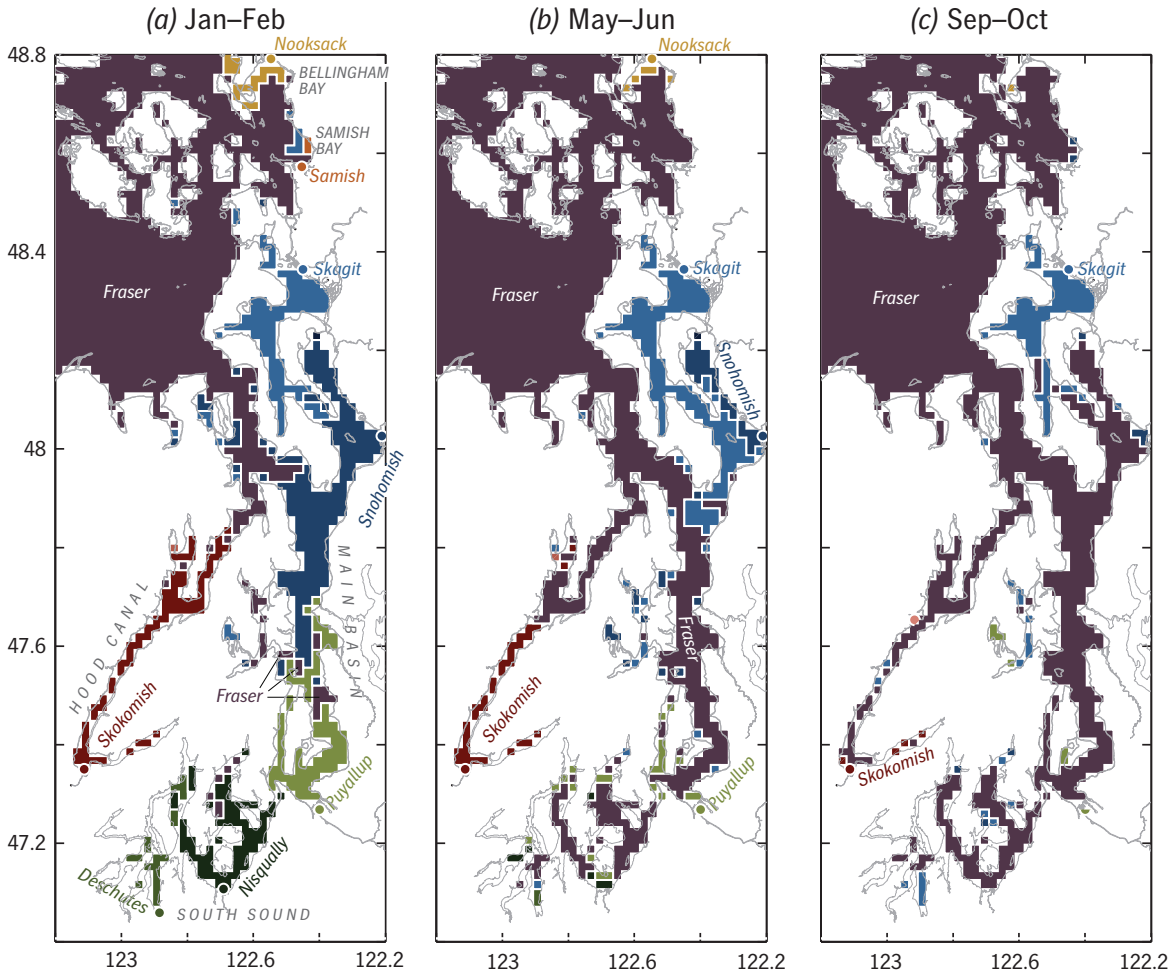


Figure 8. River contributing the largest fraction of total freshwater to each point in Puget Sound, in three two-month averages (winter, late spring/early summer, late summer) as in Fig. 7. Results are gridded at 2 km resolution. Rivers are color-coded as in Fig. 1, and major contributors are labeled by name.

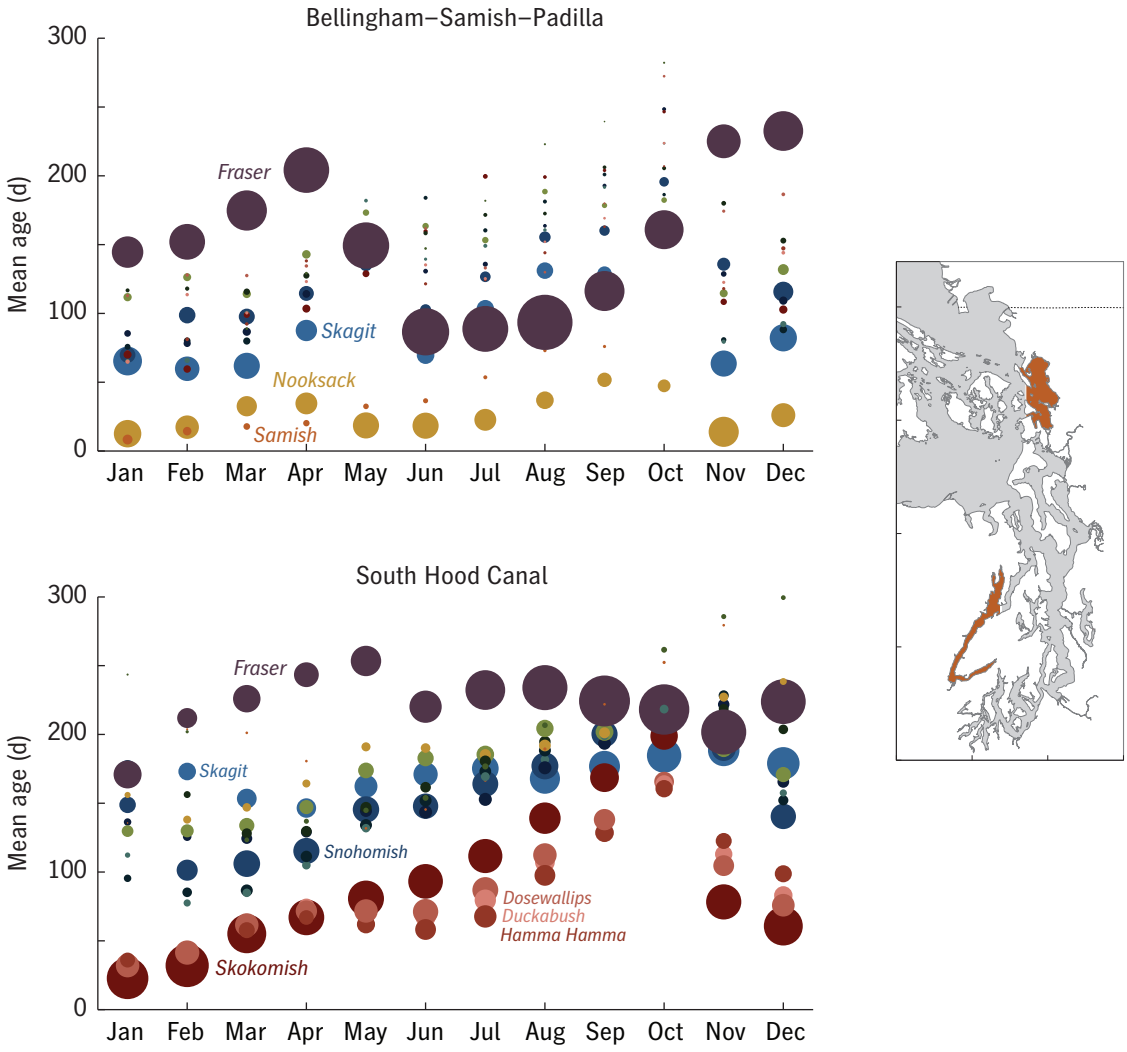


Figure 9. Mean age of the freshwater contribution from each river to two subregions, (a) the Bellingham-Samish-Padilla Bay system and (b) South Hood Canal, over a seasonal cycle. Dots are color-coded by river as in Fig. 1 and sized according to freshwater volume.

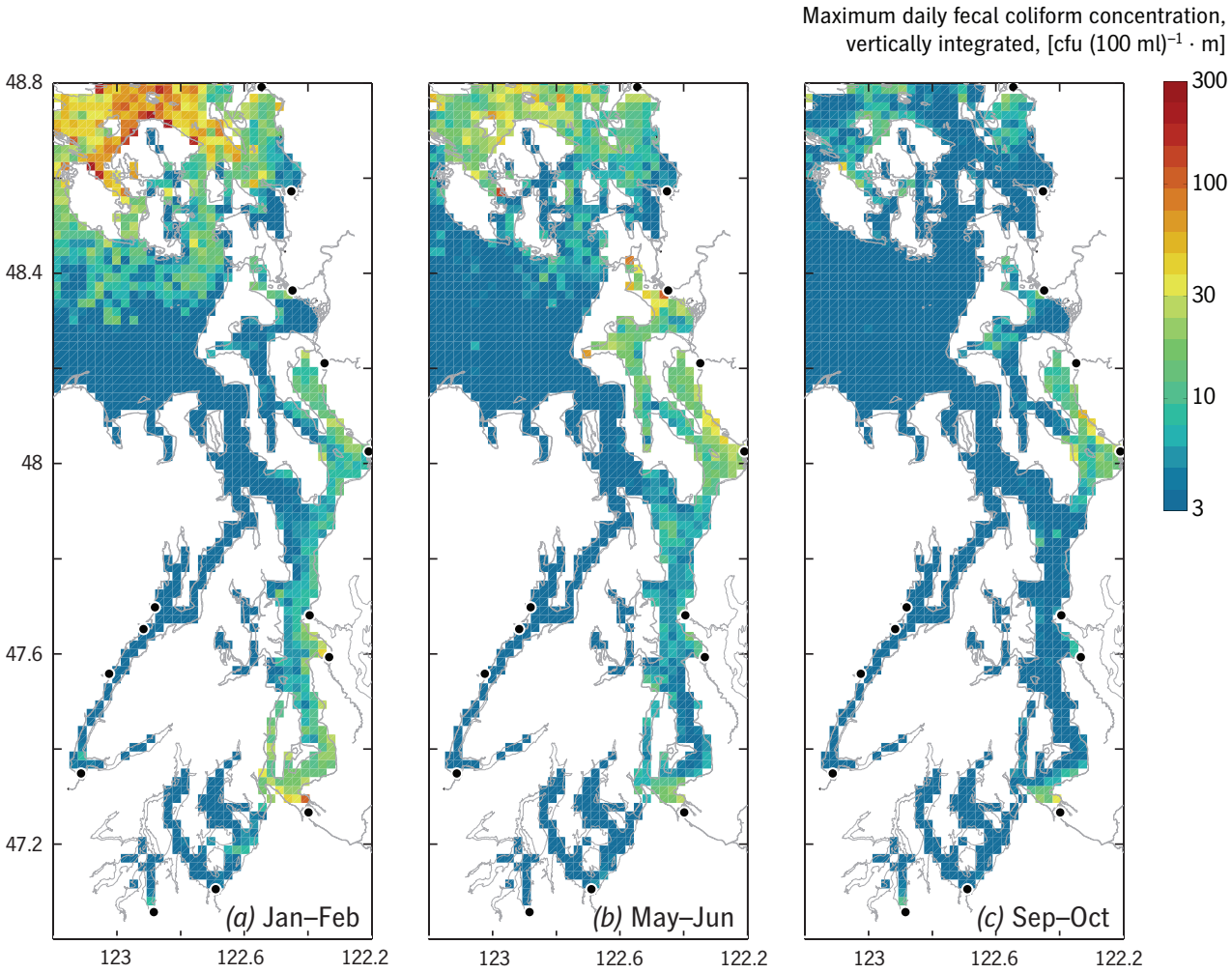


Figure 10. Fecal coliform load to Puget Sound originating in the 15 major rivers included in this study, in three seasons, (a) winter, (b) late spring/early summer, (c) late summer. For each season the maximum daily pathogen count is shown, vertically integrated (colony forming units per unit area, not per unit volume).

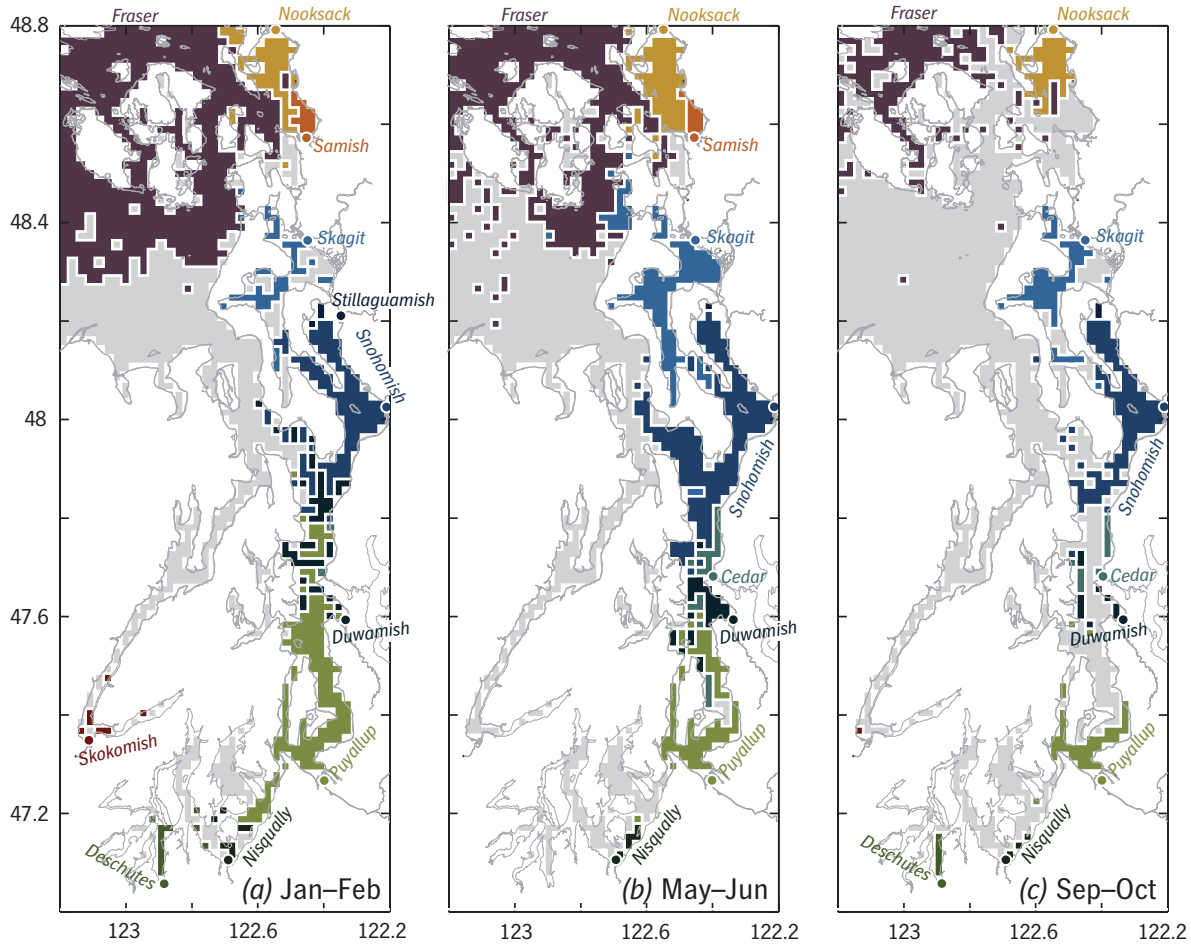


Figure 11. River contributing the largest fraction of fecal coliform, gridded at 2 km resolution, in three seasons: compare Fig. 8. Areas with maximum daily concentration < 3 cfu (100 ml)–1 m (the low end of the scale in Fig. 10) are grayed.

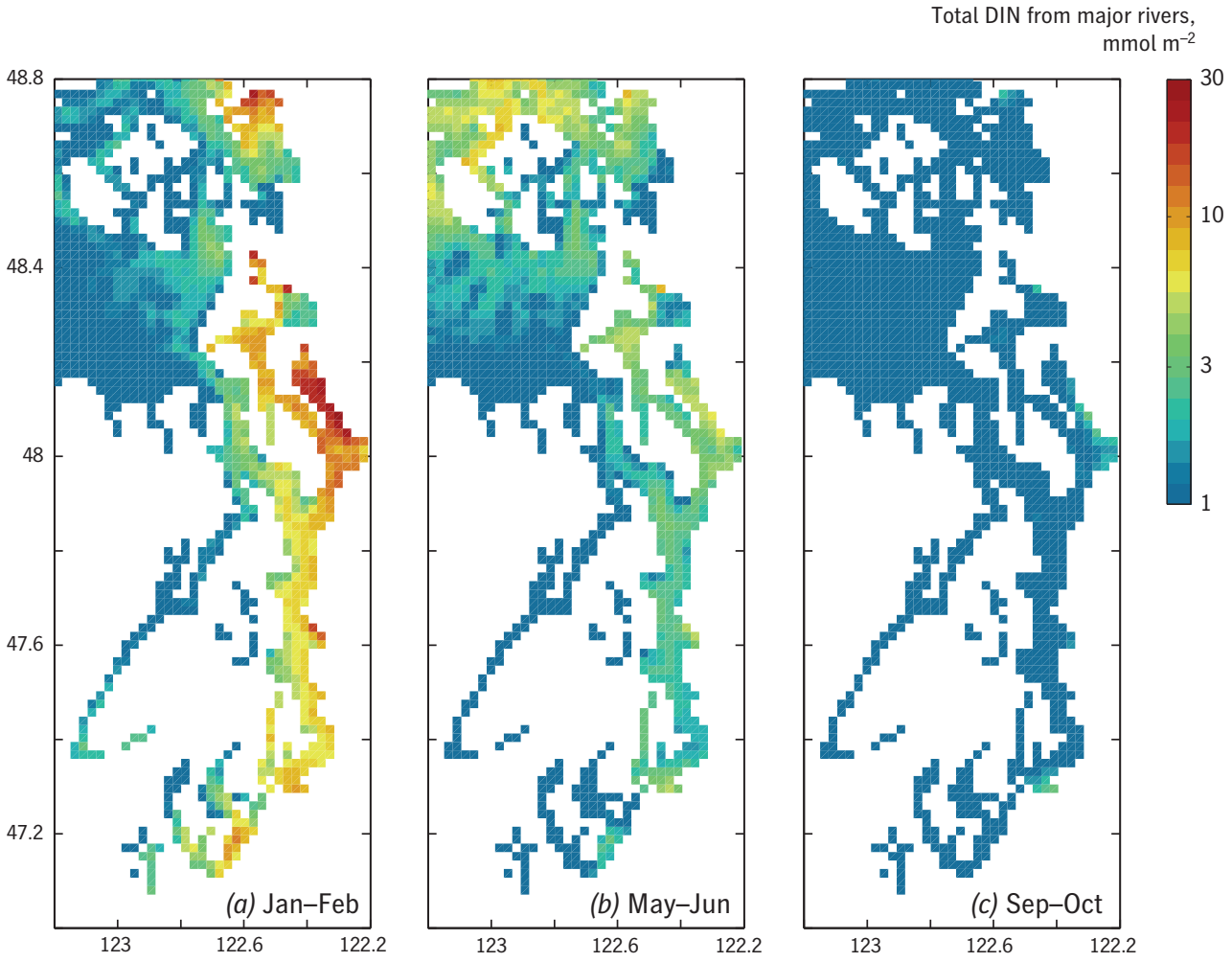


Figure 12. Mean distribution of dissolved inorganic nitrogen supplied by the 15 major rivers included in this study, averaged over three seasons. Note that concentrations are vertically integrated (mmol N per unit area, not per unit volume).

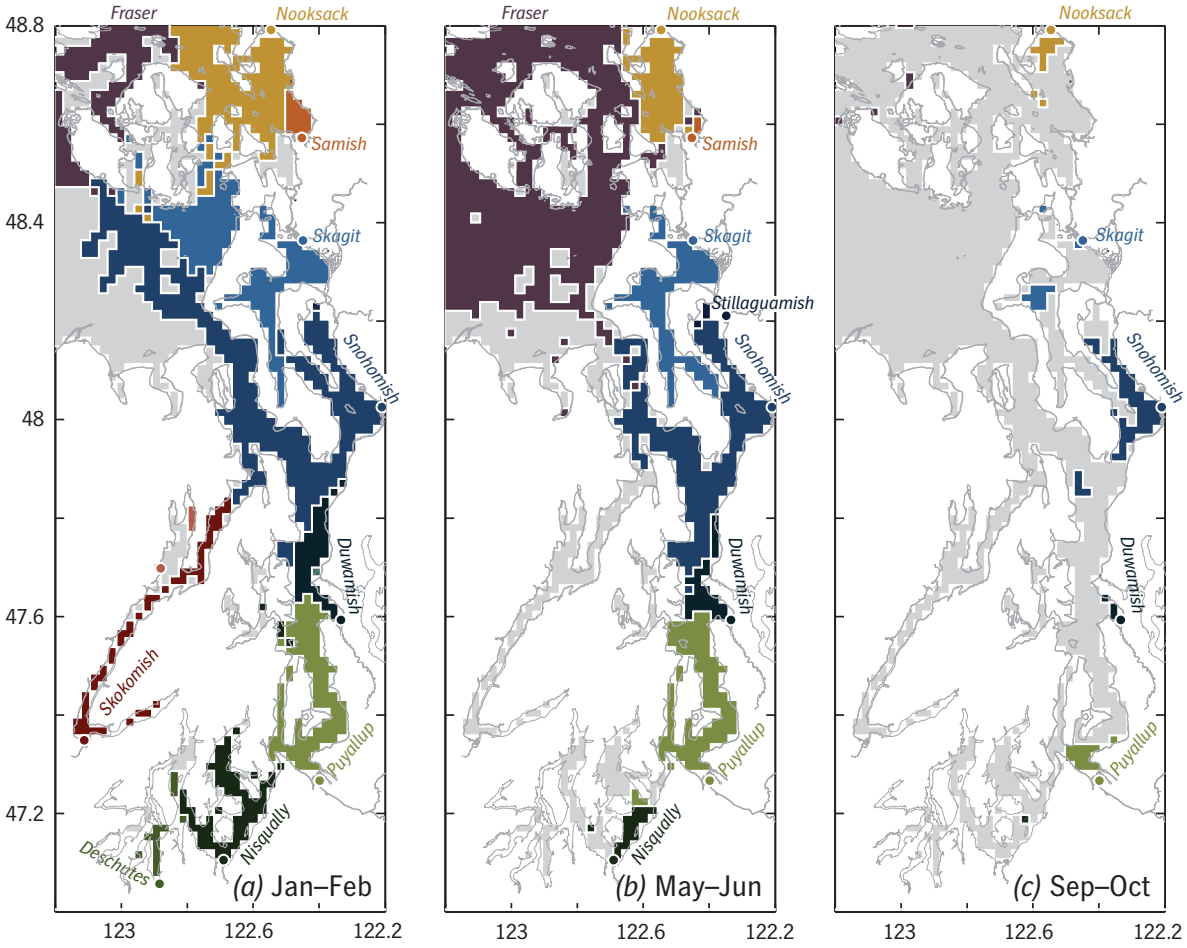


Figure 13. River contributing the largest fraction of DIN, gridded at 2 km resolution, in three seasons: compare Figs. 8, 11. Areas with integrated mean concentration < 1 mmol m–2 (the low end of the scale in Fig. 12) are grayed.

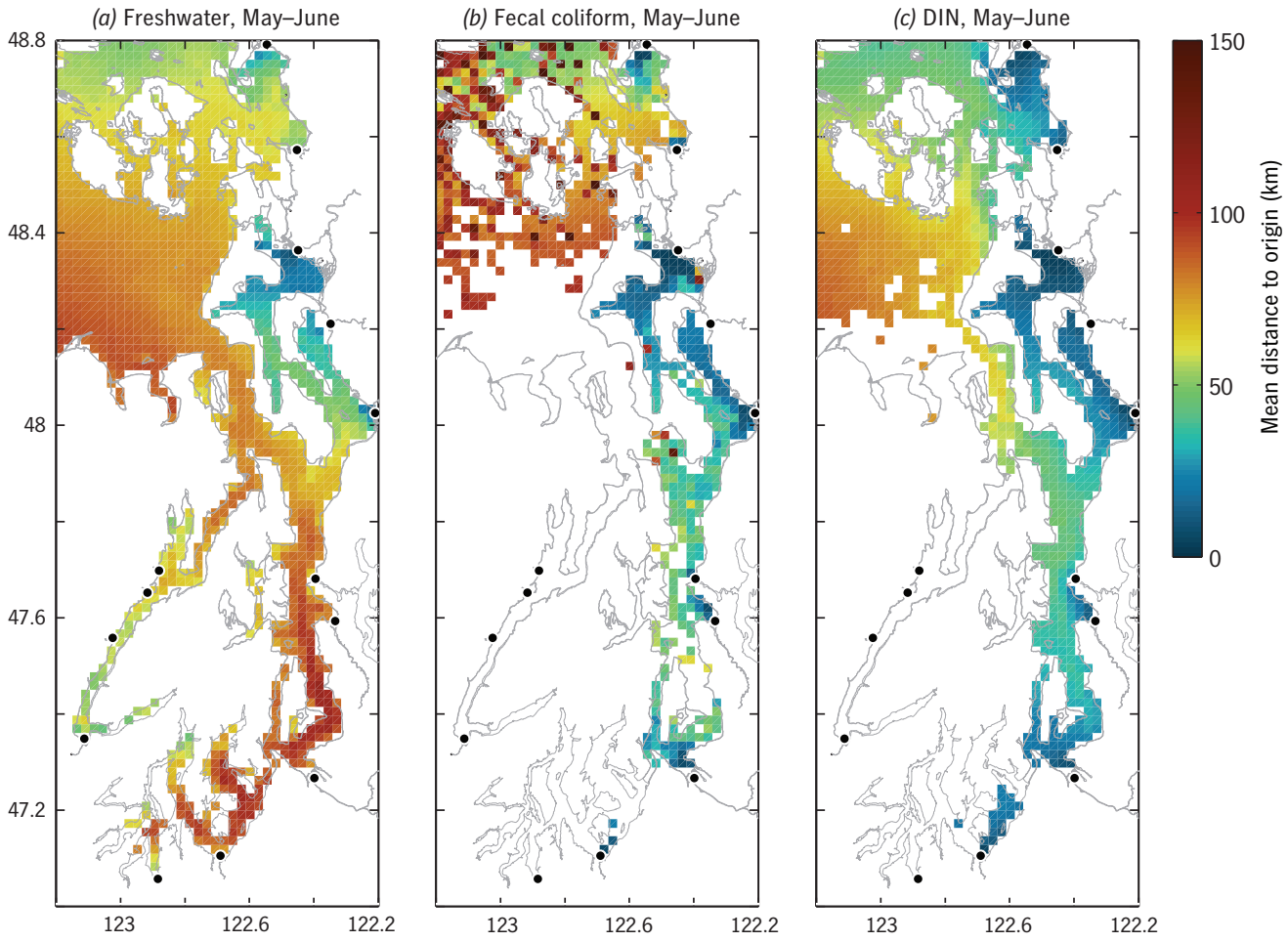


Figure 14. Mean distance to river of origin in spring/early summer, for freshwater (compare Fig. 8b), fecal coliform (compare Fig. 11b), and DIN (compare Fig. 13b).